Fragmentation of the expanding self-gravitating shell

Cardiff Univerzity: R. Wünsch, A. P. Whitworth, T. Bisbas
Astronomical Institute AV ČR Prague: J. Palouš, J. E. Dale, S. Ehlerová
ITA Heidelberg: R. Klessen, R. Banerjee

Outline:

1. Motivation from observations

   (HI shells and super-shells, Collect and Collapse model of SF)

2. Analysis of gravitational instability

   (dispersion relation, MS of fragments, momentum driven shell)

3. Numerical code

   (tree gravity solver for Flash)

4. Results from simulations

   (3D MDS simulations, cmp to SPH)

Motivation 1: HI shells and supershells

- $r \sim 10$ pc - 2 kpc, $v_{\rm exp} \sim 5 - 30$ km/s, $E \sim 10^{51} - 10^{53}$ erg
- observed in MW (Heiles, 1979; McClure-Griffiths et al., 2002), LMC (Kim, 1998), SMC (Stanimirovic, 1999), M31, M33, . . .
- origin: OB stars (fossils of expanding HII regions), ecnounter with HVC or dwarf galaxy, GRB, turbulence and instabilities in ISM

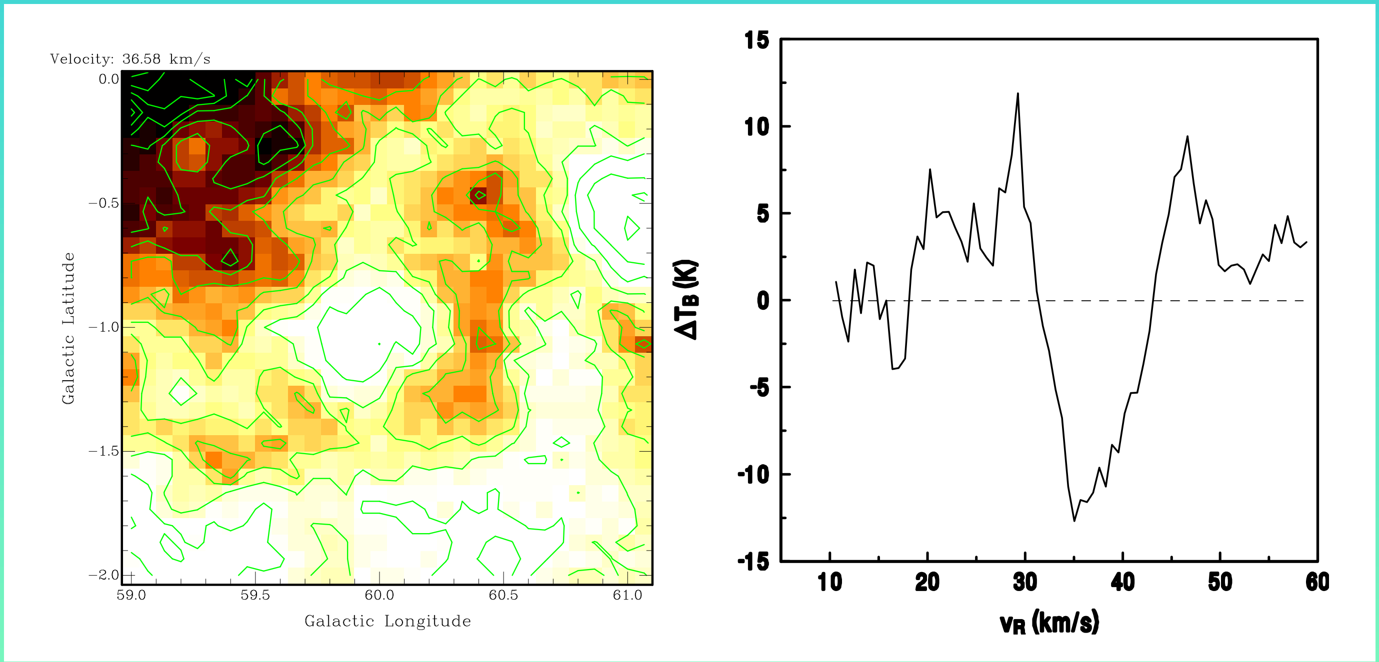

Motivation 1: HI shells and supershells 2

- TSF, disk - halo connection
- statistical study: automatic search for HI shells in Leiden-Dwingeloo survey (Ehlerová et al., 2005)

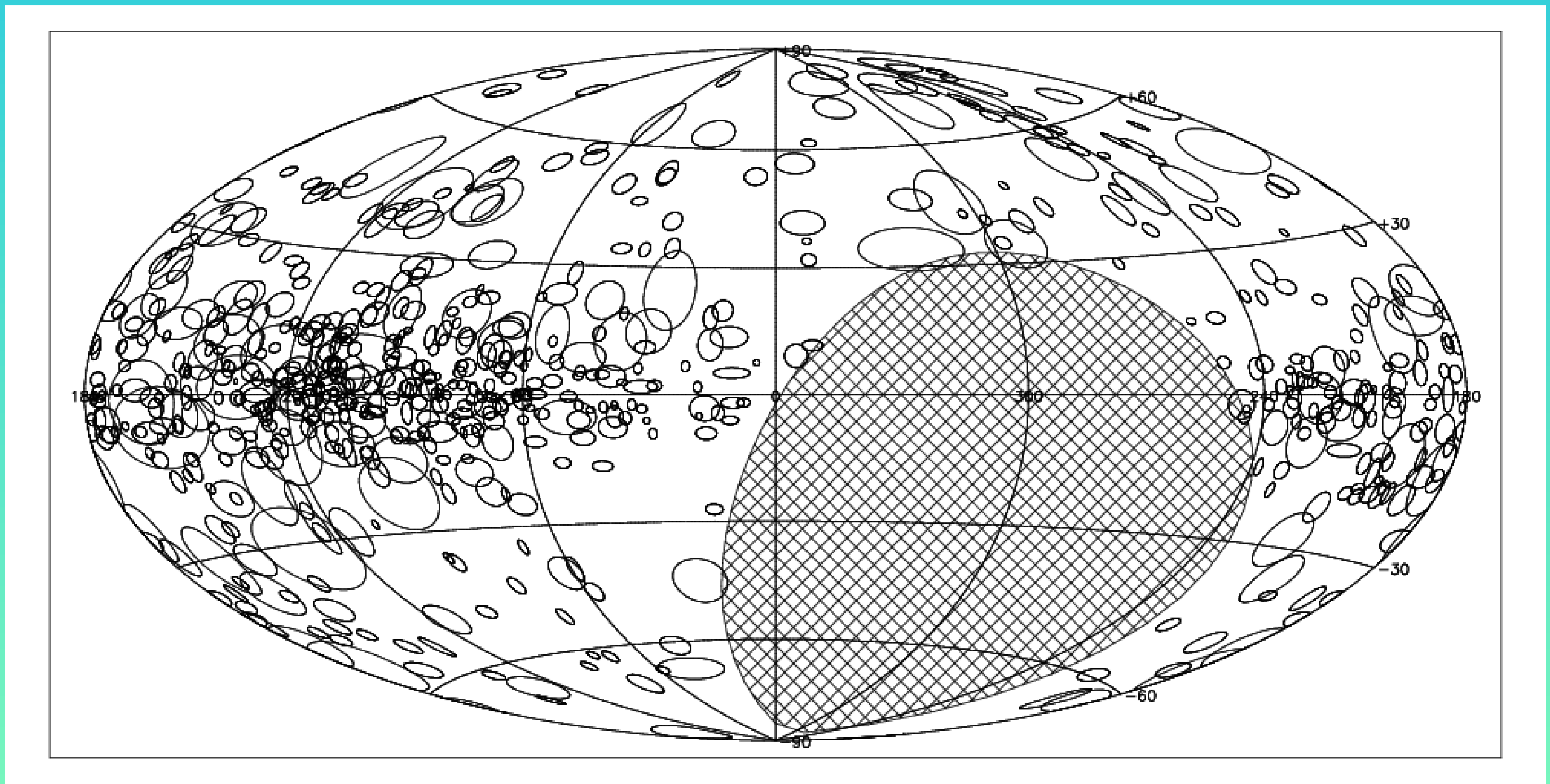

Motivation 2: Collect and collapse

- C&C (Elmegreen & Lada, 1977): SF at peripheries of HII region
- gravitation instability of material accumulated between IF and SF
- massive stars can be formed → self-propagating SF

- HII region Sh 104 (Deharveng et al., 2003)
  - ▷ *contours: thermal radio continuum (1.46 GHz)*
  - ▷ *red: mid-IR emmision (dust - PAHs)*
  - ▷ *turquoise: ionized gas*
- UC HII region in the dust ring (left)
- coincides with IRAS 20160+3636 point source - exciting embedded cluster

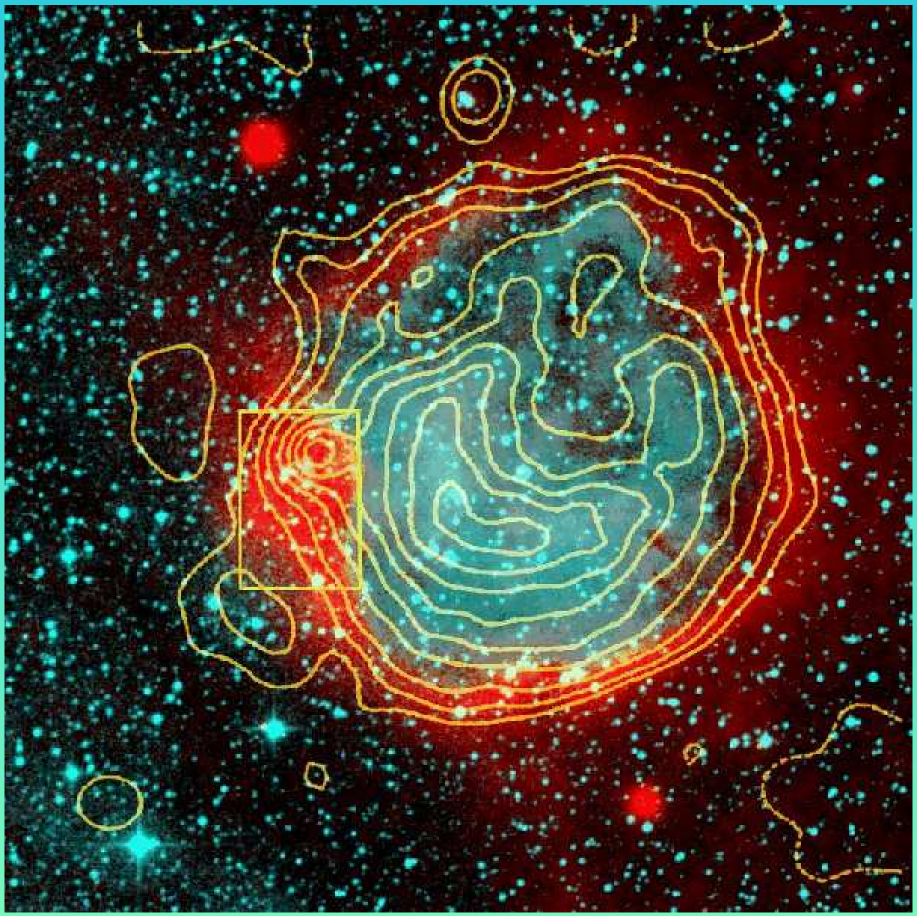

Motivation 2: Collect and collapse 2

- observations of molecular lines of Sh 104 show fragmentation
- 17 C&C candidate regions suggested by Deharveng (2005)

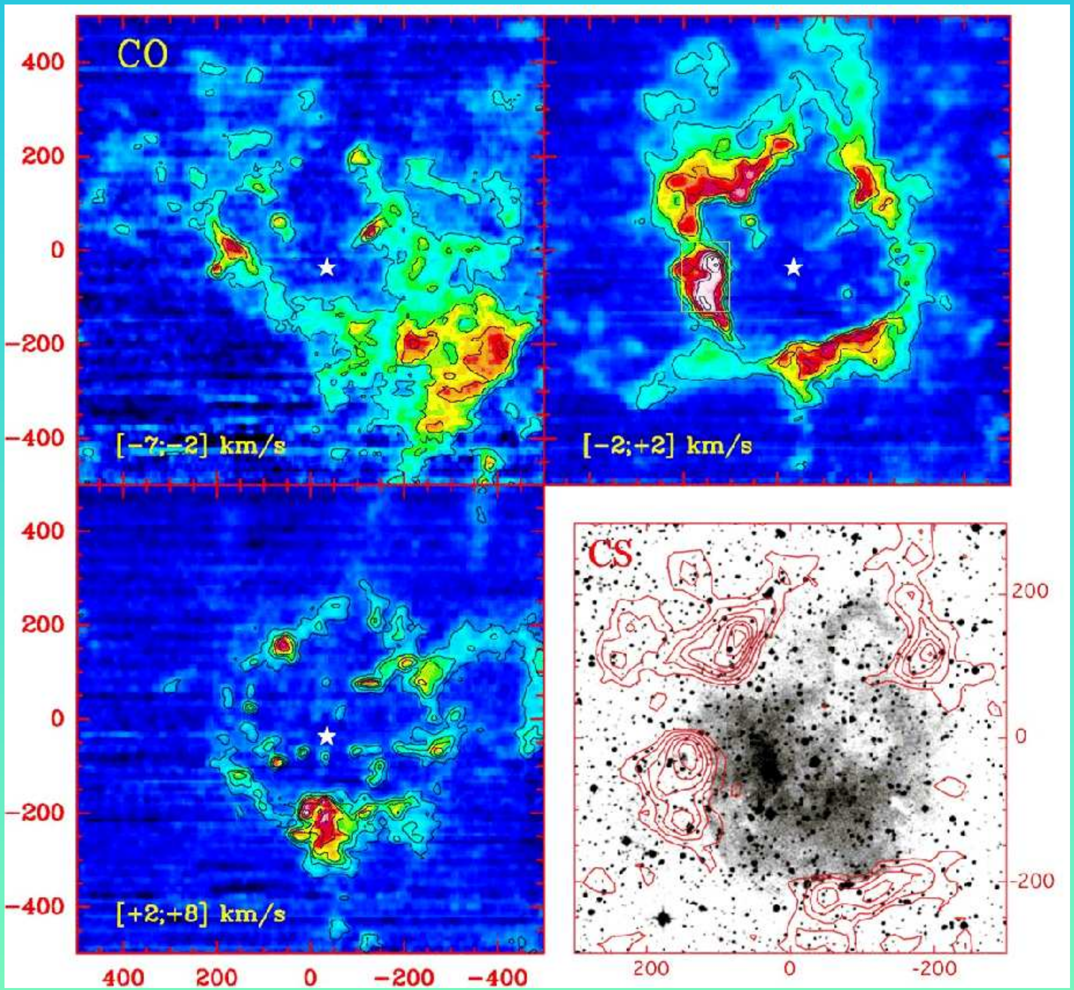

Gravitational instability

- GI in the expanding accreting shell studied analytically by Visniac (1983), Whitworh et al. (1994) and Elmegreen (1994)
- spherical thin shell expanding into homogeneous medium
- liniearized perturbed 2D HD eqs in the shell:

pressure gravity stretching accretion

$$\Sigma_0 R \frac{\partial \mathbf{\Omega}}{\partial t} = -c_s^2 \nabla \Sigma_1 + \Sigma_0 \nabla \Phi_1 - \Sigma_0 \mathbf{\Omega} V - 3\Sigma_0 \mathbf{\Omega} V$$

$$\frac{\partial \Sigma_1}{\partial t} = -\Sigma_0 R \nabla_{\mathrm{T}} \cdot \mathbf{\Omega} - 2\Sigma_1 \frac{V}{R}$$

stretching

$$\nabla^2 \Phi_1 = 4\pi G \Sigma_1 \delta(r - R)$$

Dispersion relation

- stability of mode with angular wavenumber $\eta = kR$ analysed
  $\longrightarrow$ dispersion relation:

$$\omega(\eta) = -\frac{3V}{R} + \sqrt{\frac{V^2}{R^2} + \frac{2\pi G \Sigma_0 \eta}{R} - \frac{c_s^2 \eta^2}{R^2}}$$

- the most unstable wavelength: $\eta_{\max} = \frac{\pi G \Sigma_0 R}{c_s^2}$
- fragmentation integral: $I_f(\eta, t) = \int_{t_g}^{t} \omega(\eta, t')dt'$

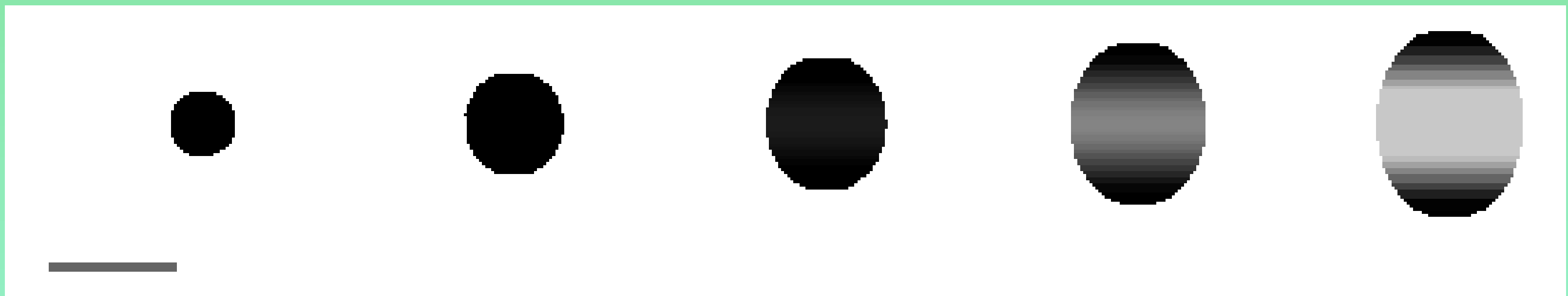

($2\frac{1}{2}D$ shell simulations by Ehlerová et al., 1997)

Mass spectrum of fragments

- fragmentation integral used as statistical meassure of number of fragments developed at wavenumber η

$$dN \propto I_f(\eta, t)\eta^2 d\eta$$

$$\eta \rightarrow m\text{: } m = \pi(\pi\eta/R)^2\Sigma \Rightarrow dN \propto m^{-\alpha} dm$$

▷ *scale-free inst.* $(\omega = \text{const})$*:* $\alpha = 2$

▷ *Jeans inst.* $(\omega = \sqrt{4\pi G\rho - c_s^2 k^2})$*:* $\alpha = 2$

▷ *thin layer:* $\alpha = 2.25$

▷ *thin expanding shell:* $\alpha = 2.35$

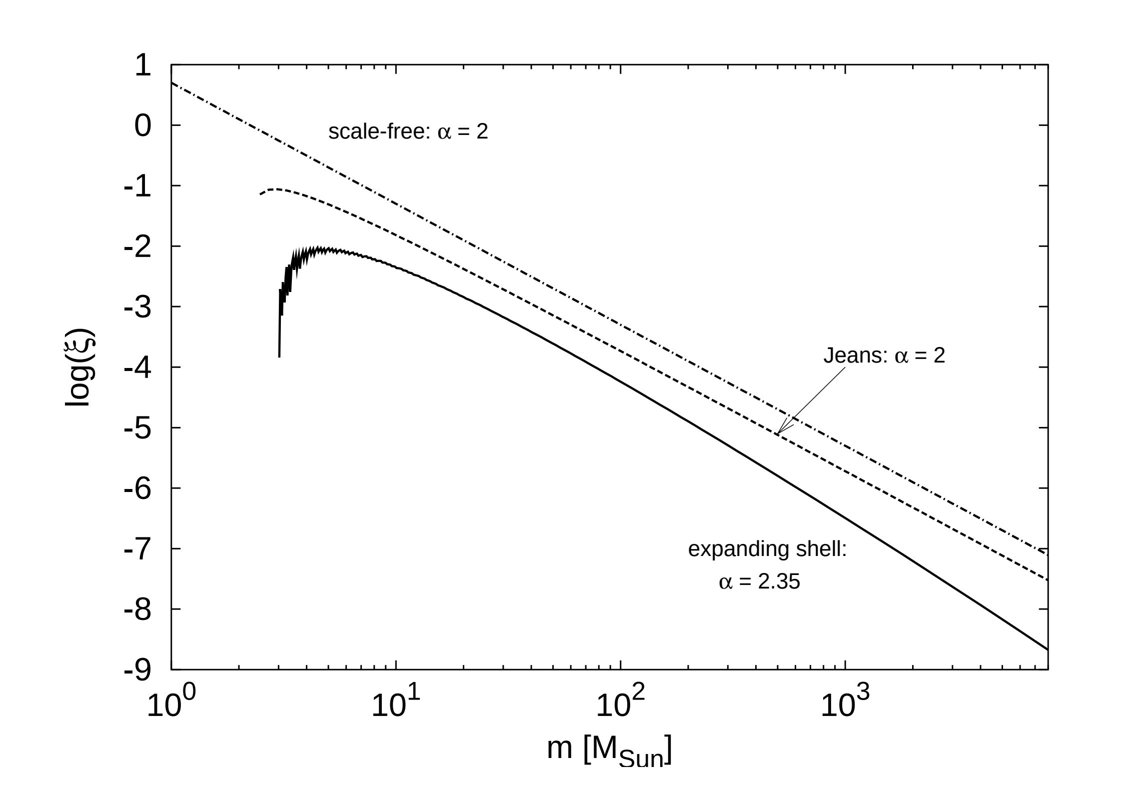

Expanding shell instabilities

- gravitational instability (long time-scale)
- dynamical inst. (short time-scale; Vishniac, 1983; 1994)
- Rayleigh-Taylor instability

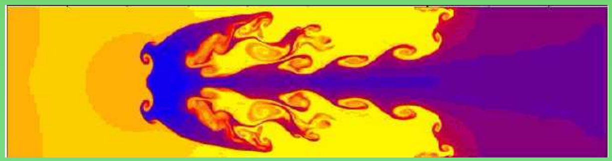

- magnetic field:

  Parker inst. (Parker 1966)

  Wardle inst. (Wardle, 1990)

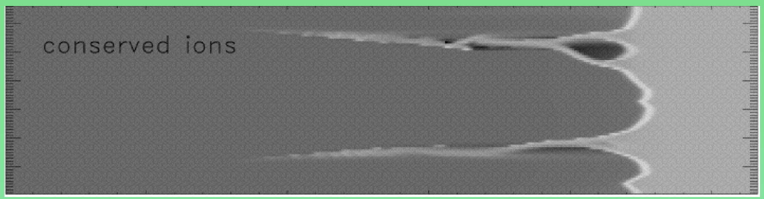

- ionized shell instability (Garcia-Segura & Franco, 1996)

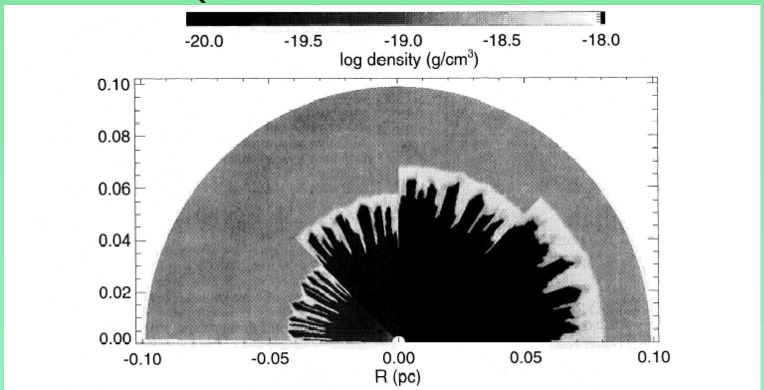

FIG. 6.—Evolution of the I-S front instability for a case with constant density (model UC32). The cooling cutoff is 10^3 K, and the time step is 5×10^3 yr. The ambient medium has $n_0 = 10^5$ cm^{-3} and $T_0 = 100$ K, and the stellar flux is $F_\star = 10^{48}$ s^{-1}. This model is equivalent to the very early stages of model S32, shown in Fig. 8.

Momentum driven shell

- expanding HII region studied numerically e.g. by Mac Low et al. (2007) and Dale et al. (2007)
- we concentrate on grav. inst. $\rightarrow$ momentum driven shell
- parameters: M, T, R_0 and $V_0 \rightarrow R_{\rm max}$
- important time-scales:

free fall time: $t_{\rm ff} = \frac{\pi R_{\rm max}^{3/2}}{2(GM)^{1/2}}$

grav. inst. time: $t_{\rm grav} = \frac{2\pi}{\omega} = \frac{8\pi R_{\rm max}^2 c_s}{GM}$ where

$$\omega_{\rm max} = -\frac{3V}{2R} + \sqrt{\frac{V^2}{4R^2} + \frac{\pi^2 G^2 \Sigma_0^2}{c_s^2}} = \frac{GM}{4 c_s R_{\rm max}^2}$$

is growth rate of the most unstable wavelength at $R_{\rm max}$ with wavenumber:

$$\eta_{\rm max} = \frac{\pi G \Sigma R_{\rm max}}{c_s^2} = \frac{GM}{4 c_s^2 R_{\rm max}}$$

Momentum driven shell 2

- enough time for fragmentation: $$\frac{t_{\rm ff}}{t_{\rm grav}} = \frac{(GM)^{1/2}}{16 c_s R_{\rm max}^{1/2}} = \frac{\eta_{\rm max}^{1/2}}{8} \gtrsim 1$$

$$\Rightarrow \eta_{\rm max} \gtrsim 64$$

- expansion of the shell: $$\Delta R \sim t_{\rm ff} c_s$$
- thin shell approximation breaks for modes $\eta > \eta_{\rm cutoff}$

$$\eta_{\rm cutoff} = \frac{2\pi R_{\rm max}}{\Delta R} = 8\eta_{\rm max}^{1/2}$$

$$\Rightarrow \eta_{\rm max} \lesssim 64$$

- 3 models: $T = 10$ K, $R_0 = 10$ pc, $R_{\rm max} = 23$ pc

$\frac{M}{[\rm M_\odot]}$	$\frac{V_0}{[\rm kms^{-1}]}$	$\eta_{\rm max}$	$\frac{t_{\rm ff}}{[\rm Myr]}$	$\frac{t_{\rm grav}}{[\rm Myr]}$	$\frac{\Delta R}{[\rm pc]}$	$\eta_{\rm cutoff}$
10^4	1.56	11.3	25.6	60.8	5.3	26.9
2×10^4	2.2	22.6	18.1	30.4	3.8	38.1
4×10^4	3.1	45.2	12.8	15.2	2.7	53.8

Numerical model

- based on AMR code Flash
- eos effectively isothermal
- new tree-based gravity solver developed

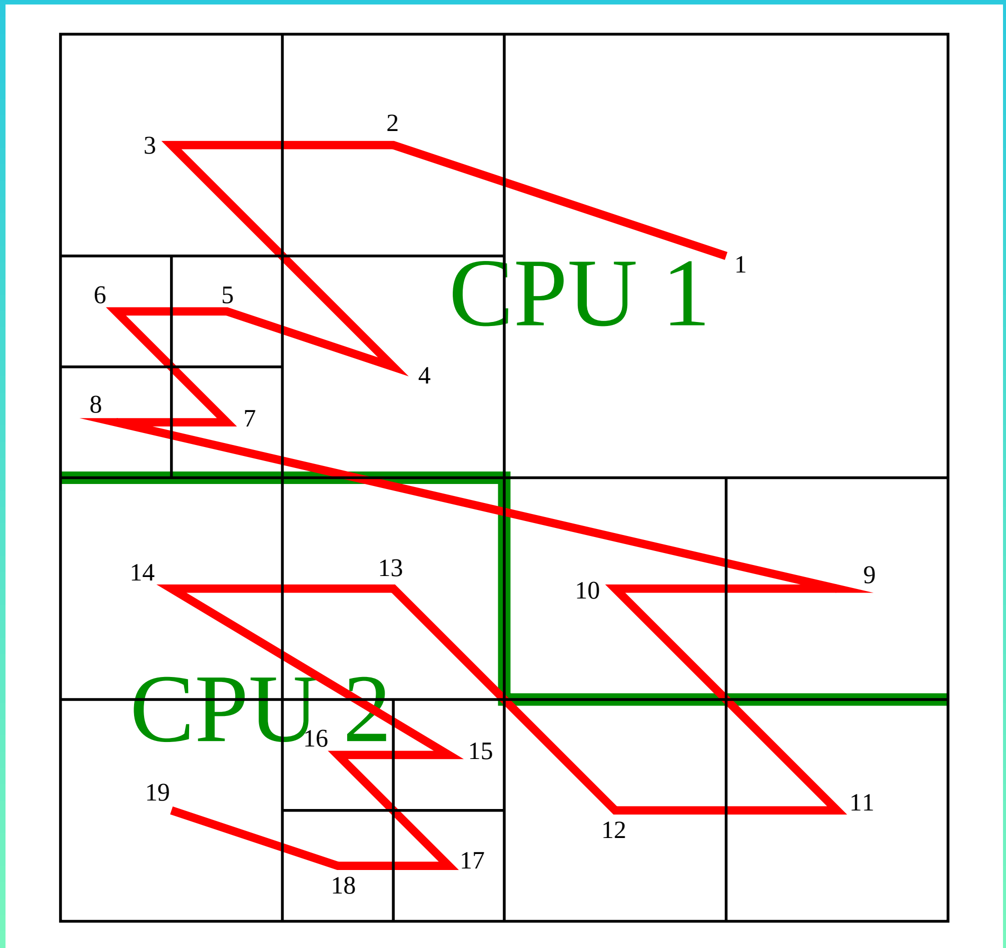

- Flash:
  - ▷ *MPI-parallel*
  - ▷ *domain decomposition - based on blocks in octal tree*
  - ▷ *load balancing - Morton curve*

Gravity tree

- octal tree in each block + global tree blocks (AMR structure)
- masses and positions of mass centers (no quadrupole moments)
- communication:
  - ▷ *whole global tree: whole*
  - ▷ *individual block trees: only to a necessary level*

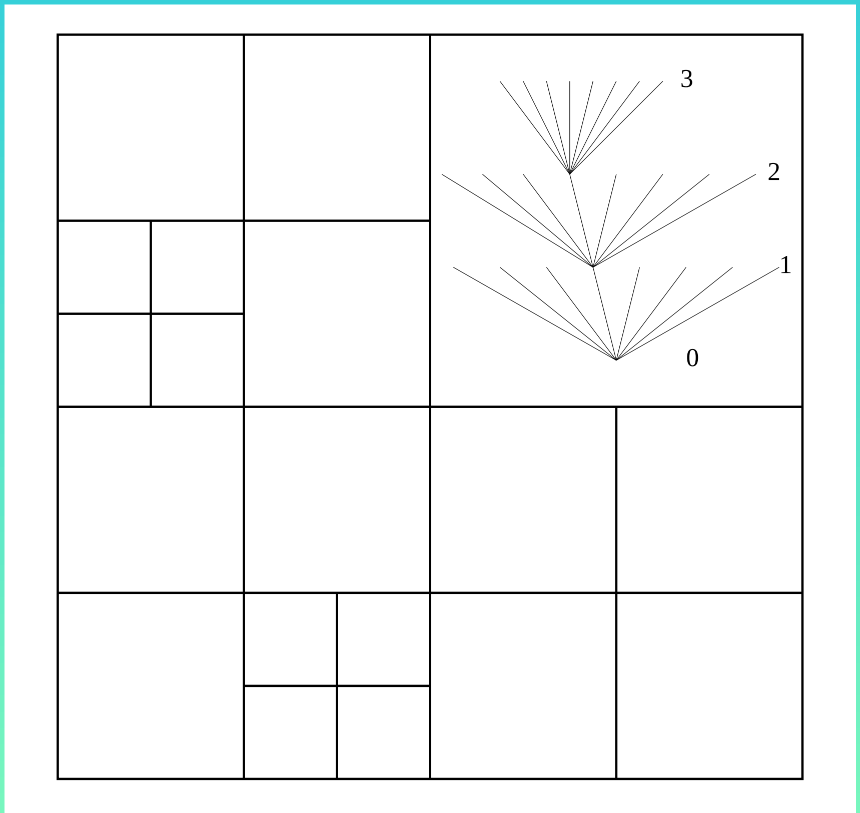

Gravity tree

- octal tree in each block + global tree blocks (AMR structure)
- masses and positions of mass centers (no quadrupole moments)
- communication:
  - ▷ *whole global tree: whole*
  - ▷ *individual block trees: only to a necessary level*

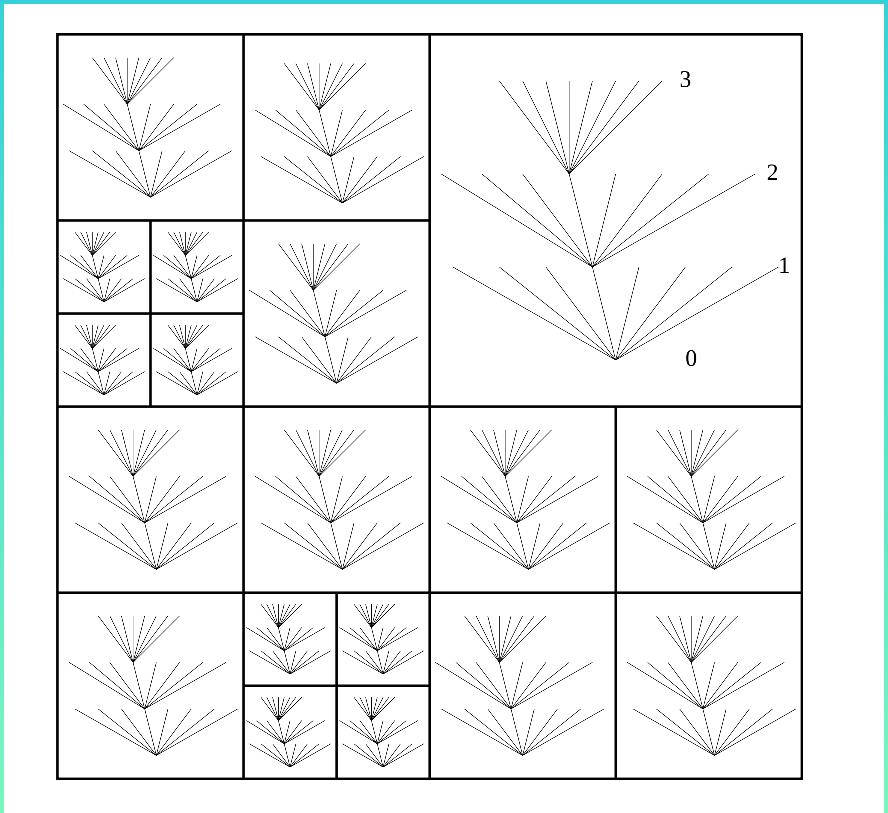

Gravity tree

- octal tree in each block + global tree blocks (AMR structure)
- masses and positions of mass centers (no quadrupole moments)
- communication:
  - *whole global tree: whole*
  - *individual block trees: only to a necessary level*

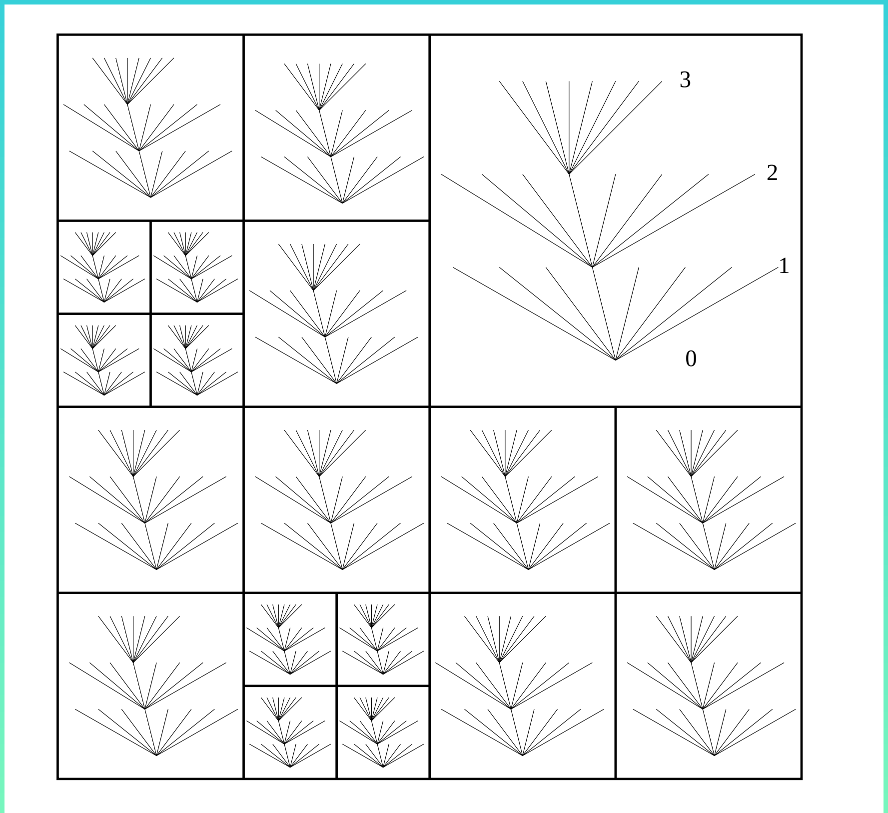

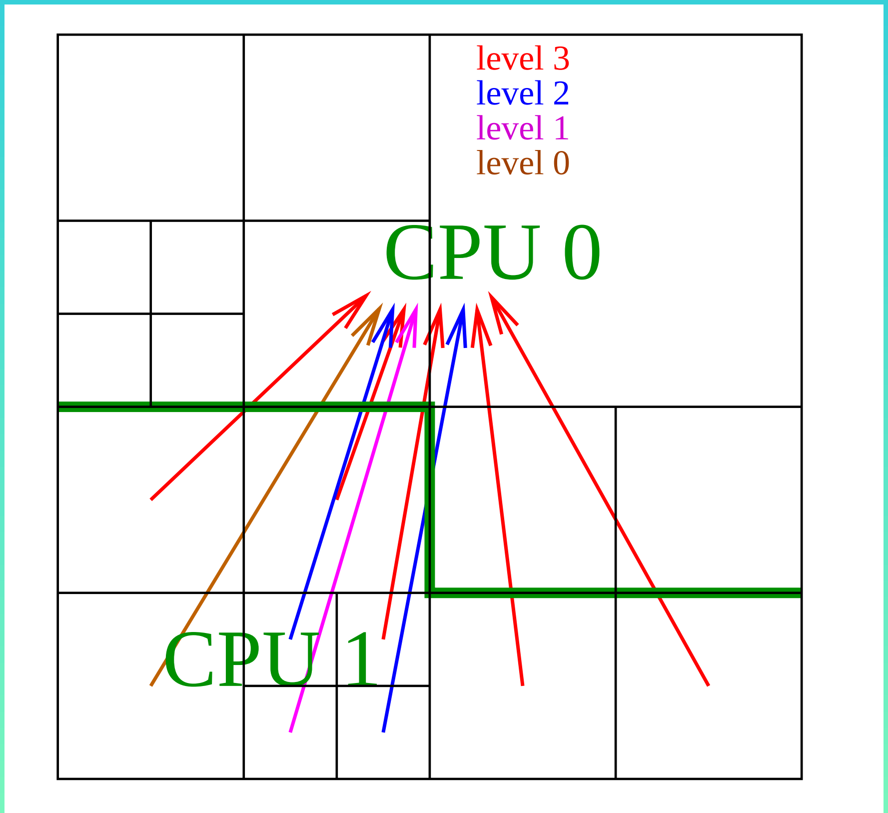

Tree in RAM

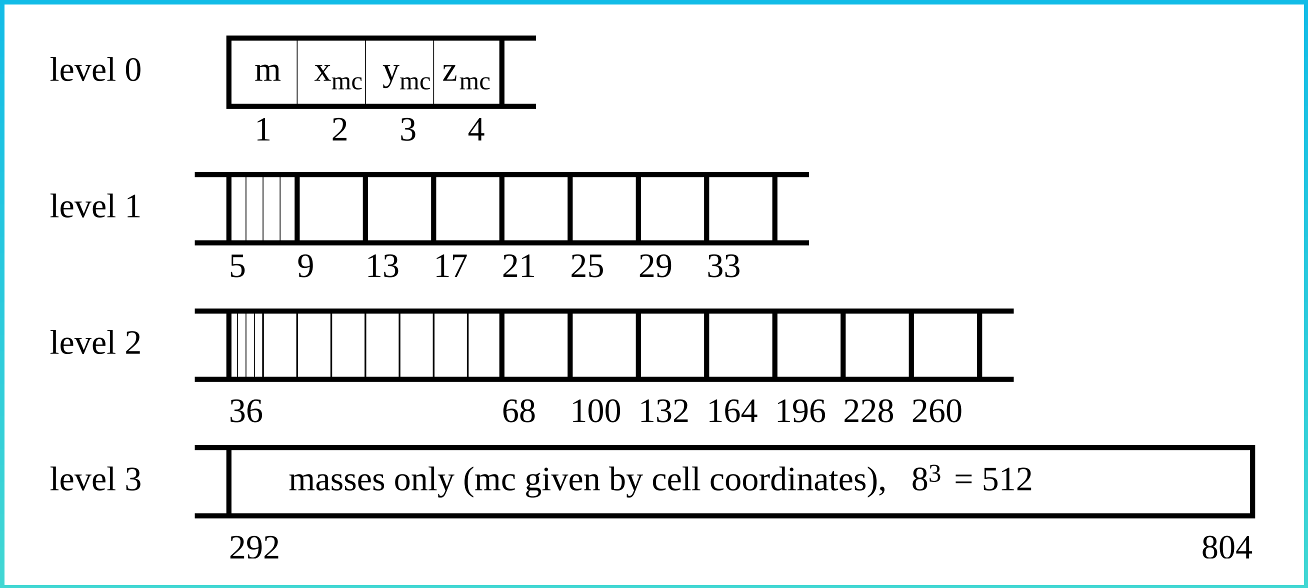

L . . . number of the lowest level (typically 3)

$$\text{Tree size} = 8^L + 4\sum_{i=0}^{L-1} 8^i = 8^L + 4\frac{8^L - 1}{7}$$

tree nodes identified by multi-index - integer array of size L: (l_1, l_2, l_3); $l_i =$

- *1-8 . . . number of node on i-th level*
- *0 . . . multi-index (i.e. node) is of level i-1*

MDS simulation

- parameters:
  - ▷ $M = 2 \times 10^4$ *M*$_\odot$
  - ▷ $T = 10$ *K*
  - ▷ $R_0 = 10$ *pc*
  - ▷ $V_0 = 2.2$ *km/s*
  - ▷ $R_{\max} = 22.9$ *pc*
  - ▷ $\eta_{\max} = 22.6$
  - ▷ $t_{\mathrm{ff}} = 18.1$ *Myr*
  - ▷ $t_{\mathrm{grav}} = 30.4$ *Myr*
  - ▷ $\eta_{\mathrm{cutoff}} = 38.1$
- code performance:
  - ▷ *grid virtualy* 192^3
  - ▷ $t_{\mathrm{end}} = 31.7$ *Myr*
  - ▷ $12 CPUs$*, 31 hrs, 286 dt*
  - ▷ *gravity . . . 82%*
    - build tree . . . 0.5%
    - communication . . . 11%
    - potential . . . 71%
  - ▷ *hydro . . . 11%*

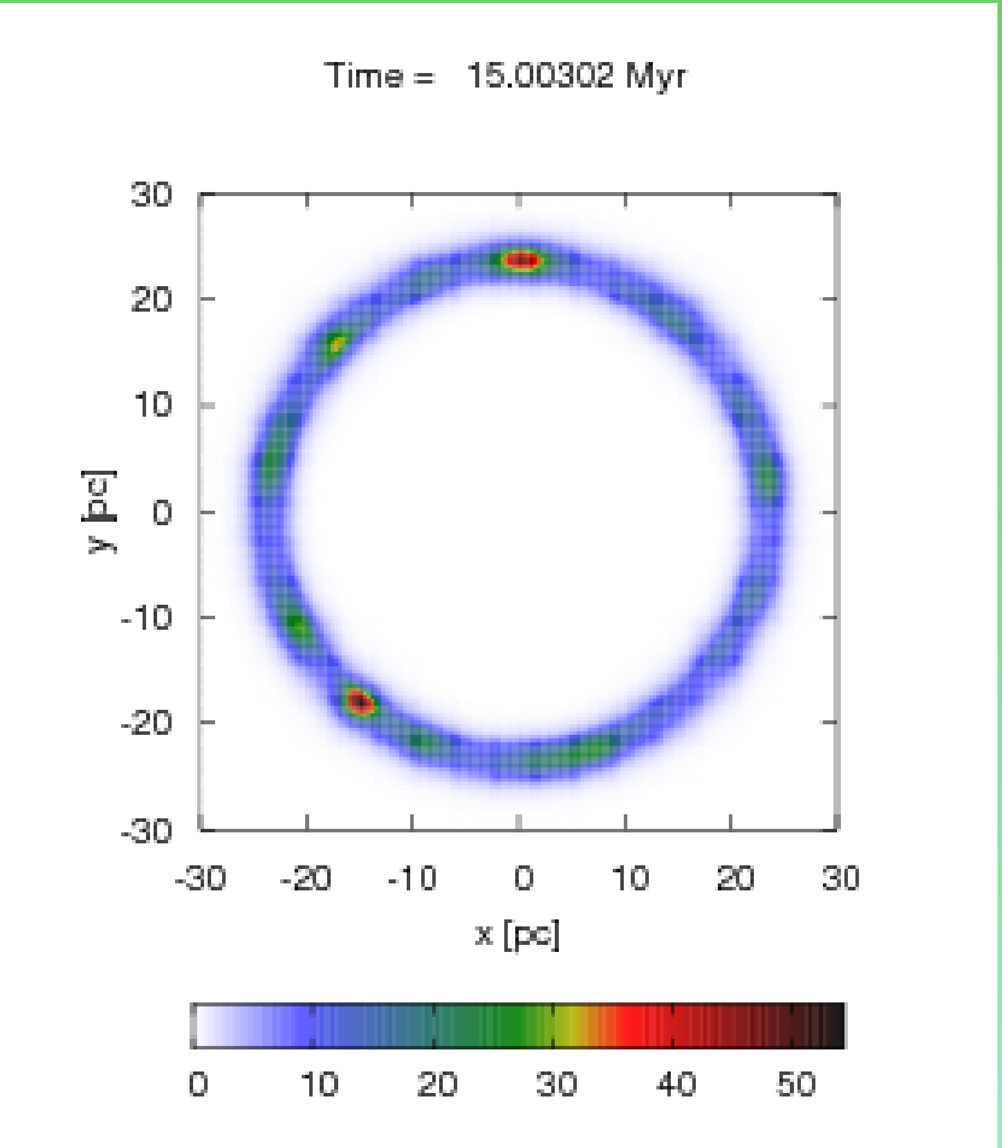

Analysis of mode growth

- surface density decomposed into spherical harmonics $\rightarrow C_l$
- perturbation growth rate at given $l \equiv \eta$: $\omega = \dot{C}_l / C_l$

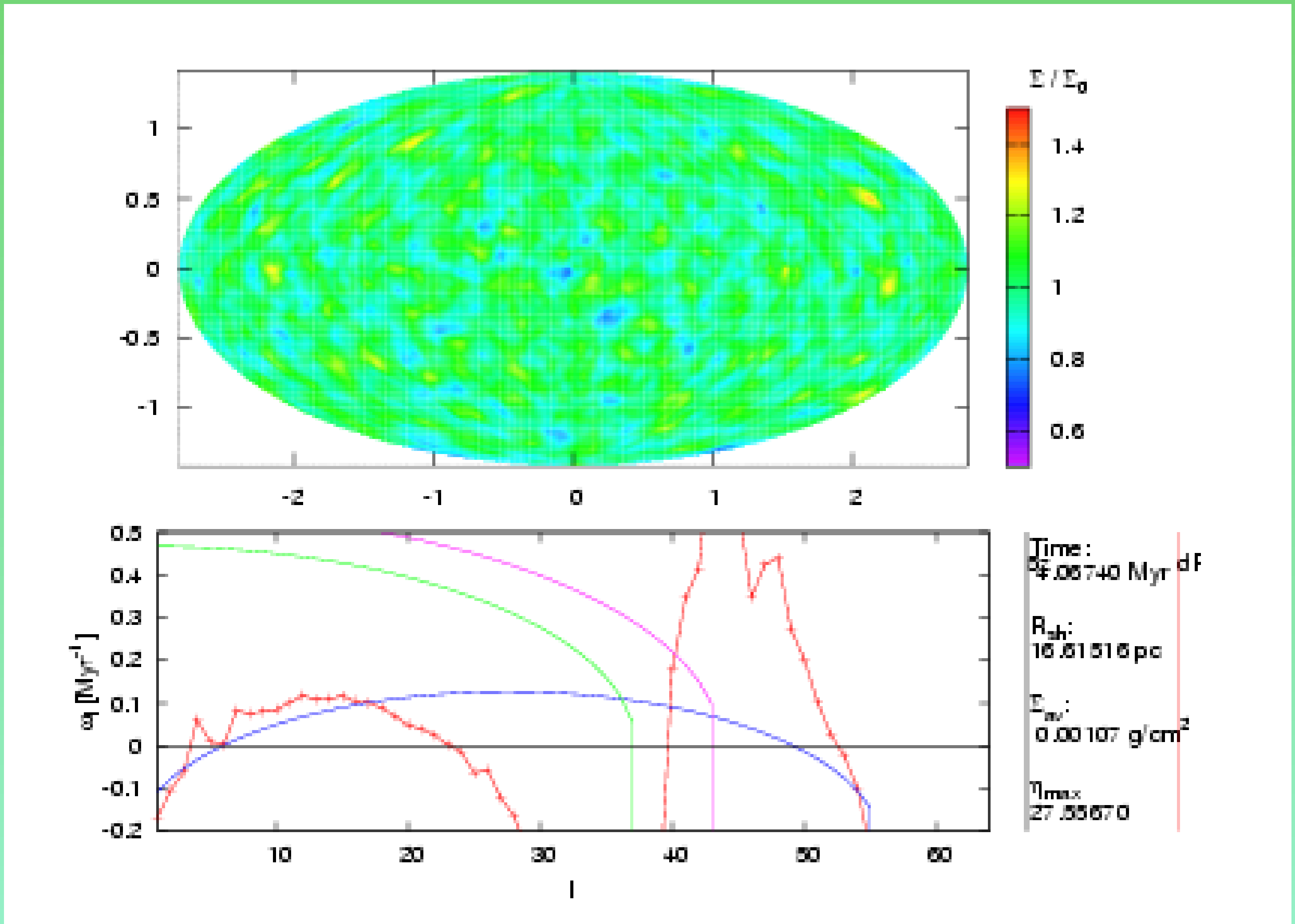

Shells with different mass

- *top right:* $M = 10^4\ M_\odot$
  $\eta_{\max} = 11.3$
- *bottom left:* $M = 2 \times 10^4\ M_\odot$
  $\eta_{\max} = 22.6$
- *bottom right:* $M = 4 \times 10^4\ M_\odot$
  $\eta_{\max} = 45.2$

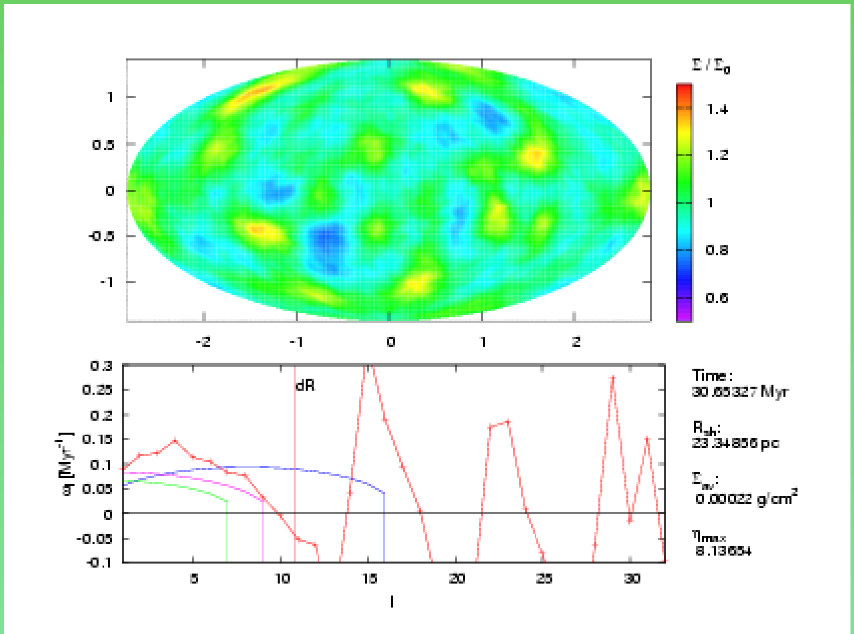

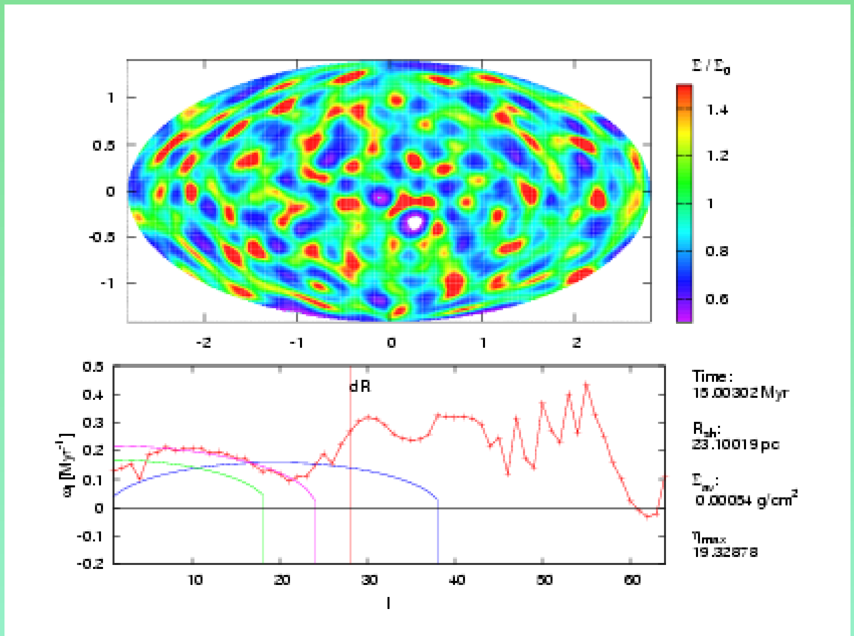

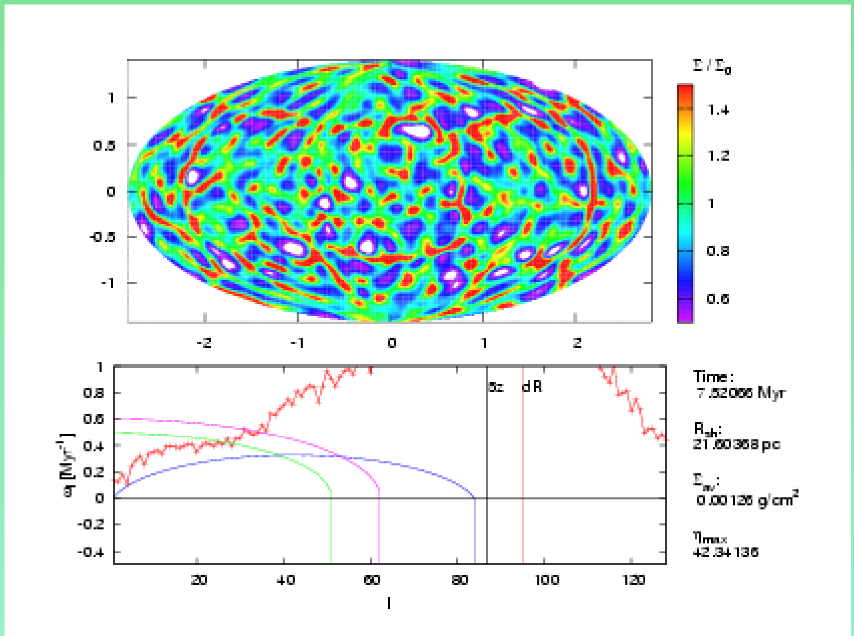

AMR vs. SPH

- left: AMR, virtually 192^3
- right: SPH, 5×10^5 particles (by J. Dale)
- fragments slightly more developed in SPH (due to IC), but growth rates are very similar

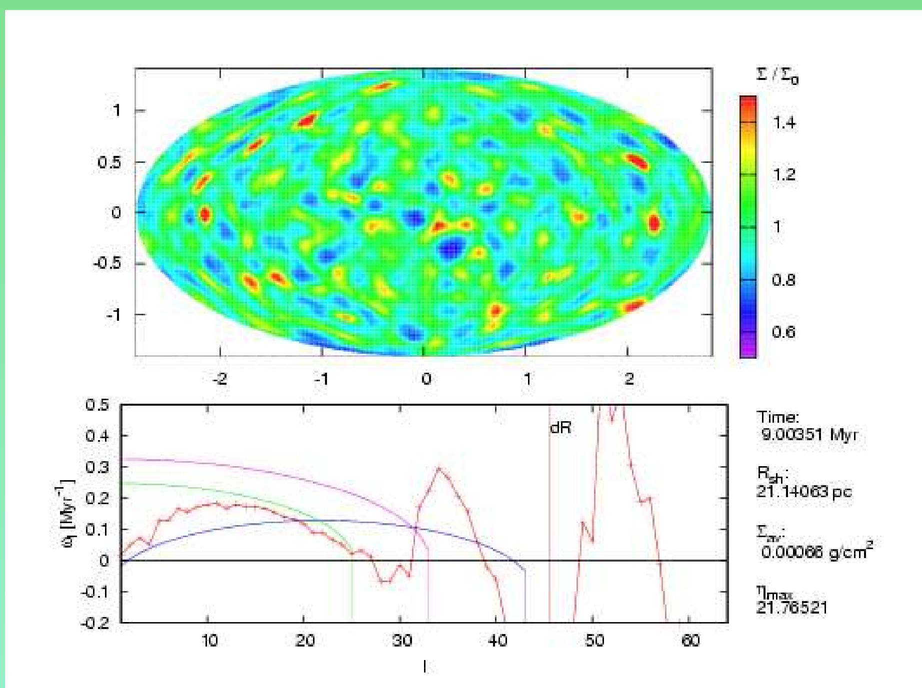

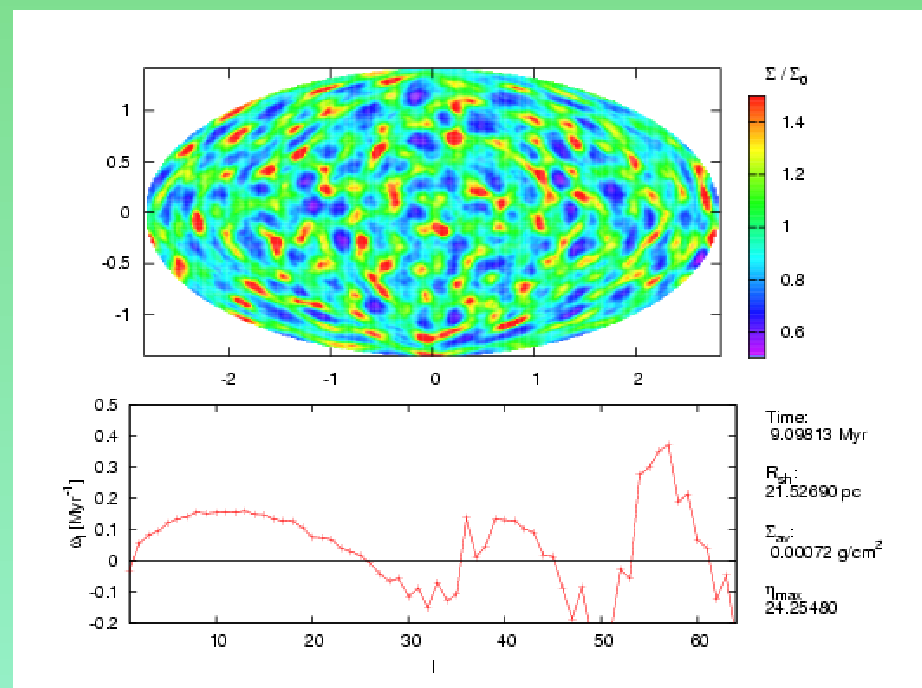

Summary

- MPI paralel tree gravity solver for Flash developed
- only narrow range of parameters where thin shell approximations applies in case of momentum driven shell
- first low-resolution runs of momentum driven shell, growth rate as a function of wavelength determined
- long wavelengths grow in agreement with analytical theory, shorter wavelength grow slower due to finite thickness of the shell
- comparisons to SPH show reasonably good agreement

References

Ehlerová, S., et al. 1997, A&A, 328, 121

ELmegreen, B. G., Lada, C. J., 1977, ApJ, 214, 725

Elmegreen, B. E., 1994, ApJ, 427, 384

Dale, J. E., Bonnel, I. A., Whitworth, A. P., 2007, MNRAS, 375, 1291

Garcia-Segura, G., Franco, J., 1996, ApJ, 496, 171

Heiles, C., 1979, ApJ, 229, 533

Kim, S., et al., 1998, Pub. Astron. Soc. Austr., 15, 132

McClure-Griffiths, N. M., et al., 2002, ApJ, 578, 176

Mac Low, M.-M., Smith, M. D., 1997, ApJ, 491, 596

Mac Low, M.-M., Toraskar, J., Oishi, J. S., 2007, ApJ, 668, 980

Parker, E. N., 1966, ApJ, 145, 811

Stanimirovic, S.; et al., 1999, MNRAS, 302, 417

Vishniac, E. T., 1983, ApJ, 274, 152

Whitworth, A. P., et al., 1994, MNRAS, 268, 291

Wardle, M. 1990, MNRAS, 246, 98